Hindawi
Journal of Sensors
Volume 2021, Article ID 5597841, 14 pages
https://doi.org/10.1155/2021/5597841

Research Article

Detection Fusion of Weak Signal under Chaotic Noise Based on Distributed System

Shengli Zhao, Lizhi Zhang, and Liyun Su

School of Science, Chongqing University of Technology, Chongqing 400054, China

Correspondence should be addressed to Shengli Zhao; zhaoshengli@cqut.edu.cn

Received 2 March 2021; Revised 23 June 2021; Accepted 9 August 2021; Published 25 August 2021

Academic Editor: Antonio Lazaro

In this paper, the problem of signal detection under chaotic noise was considered in the distributed detection fusion system. The problem which is urgent and difficult has important research value. A new detection and fusion mechanism for weak signal under chaotic noise based on a distributed system is proposed. Due to the short-term predictability of chaotic signals and their sensitivity to small disturbances, observation of each local sensor is reconstructed in phase space according to the Takens delay embedding theorem. The locally weighted regression (LOWESS) model is used to fit the observation of each local sensor in the phase space. Thus, the chaotic noise is stripped out from the observation, and the fitting error without chaotic noise is regarded as the new observation of each local sensor. Based on the new observation without chaotic noise, an optimization model aiming at minimizing the Bayesian risk of the fusion center is established. Under the condition that the observations of local sensors are conditionally independent, the fusion rule and the sensor decision rules are derived. An algorithm is proposed to obtain the fusion rule and local decision rules. The simulation results show that the proposed signal detection and fusion algorithm can effectively detect weak signals under chaotic noise background. Specifically, the fusion performance is obviously better than that of local sensors with low SNR.

1. Introduction

Weak signal is a weak quantity which is difficult to be detected. It refers to the signal with a low signal-to-noise ratio (SNR) which is submerged by noise [1, 2]. The general methods of weak signal detection include correlation test in the time domain, sampling integral method, and spectral analysis in the frequency domain [3]. These methods have been widely used in radar, communication, automation, fault diagnosis, and seismic monitoring [4–8]. With the rapid development of science and technology, it is urgent to detect weak signals in engineering applications. In many theoretical and practical problems about signal processing, complex chaotic systems exist everywhere, especially in science and engineering. There are two reasons for using chaos as a background signal, including the high-precision measurements can be realized by using the simple chaotic systems, and according to the characteristic that chaotic systems are sensitive to the initial condition, the useful signal under the background of powerful noises can be detected. At the same time, with the maturity of chaos theory and its wide application, the combination of chaos theory and the detection of weak signals has become a research trend.

In 1990, Leung and Haykin first introduced chaos theory into the field of sea clutter [9]. By the end of the 20th century, based on the characteristics of chaos, many scholars successfully extracted weak signals under chaotic noise by using neural networks and other methods [10–13]. In recent years, many scholars have done a lot of research on the weak signal under chaotic noise and put forward many effective methods. Xing et al. aimed at the problem of weak signal detection under strong noise background, introduced genetic algorithm, particle swarm optimization algorithm, and variable scale Duffing oscillator [8, 14, 15] to improve the detection accuracy, respectively. Huang et al. determined the threshold of Duffing chaotic system by studying multiscale entropy, so as to realize the detection of target signal [16]. Wang et al. proposed the fractional-order maximum correlation entropy algorithm for the prediction of chaotic time series [17]. For more methods, please refer to the literature [18–21]. All of these studies mentioned above were carried out in a single sensor observation mode, while relevant studies based on the distributed system have not been reported.

It is well known that the distributed system has better accuracy and survivability than a single sensor. Using the distributed system to detect weak signal has a broad prospect, and people usually use this method for fault diagnosis [22–24]. Grzegorz proposed a method based on deep learning to solve the defect problem of characteristic steel element through the study of multisensor data integration [25]. Li et al. proposed a new peer-to-peer distributed Kalman filtering method by studying the distributed sensor network system [26]. He established a sensor network target detection model in a nonideal channel and studied the sensor network target detection algorithm from the two perspectives of system energy consumption and system detection performance [27]. Kassam et al. proposed a generalized observation model based on the local optimal detector to detect the signal [28, 29]. For wireless sensor networks, Ciuonzo et al. proposed a generalized local optimal method to detect target signals [30, 31]. Many scholars have done in-depth research on a distributed system, especially the professor “P. K. Varshney”, and his papers are at the heart of the distributed detection. He has written a book on distributed detection and fusion, which provides an introduction to decision making in a distributed computational framework [32]. What is more, he has used numerous examples throughout the book to discusses such distributed detection processes under various different formulations and in a wide variety of network topologies. There are extensive studies on distributed detection fusion, including least-square fusion rule, large deviation analysis, Rao test, and high-order spherical-radial criterion [33–37]. In addition, some researchers have carried out distributed detection for sparse signal or weak signal and prove the superiority of the proposed methods through simulation experiments [38–40]. However, most of these studies are carried out under general noise which can be described in terms of a definite distribution. There are few reports on distributed detection and fusion under chaotic noise. That is, Su et al. conducted a research on the detection and fusion of weak pulse signals in chaotic noise background based on the local linear model, which provided a basis for this paper and subsequent research [41].

In this paper, the specific idea of weak signal detection and fusion is as follows: first of all, the observation of each local sensor was reconstructed in phase space, and the LOWESS model was used to divest the chaotic noise. Then, under the Bayes criterion, an optimization model was established based on the fitting errors. The optimal local decision rules and fusion rule were proposed. Finally, a specific algorithm was designed to solve the optimal local decision rules and fusion rule.

The structure of this paper is as follows: part 2 introduces the distributed detection model under chaotic noise based on distributed detection fusion system. Part 3 uses phase space reconstruction to strip chaotic noise. The fourth part establishes the distributed detection fusion model under the Bayes criterion. Part 5 presents the experimental simulations in different scenarios. Part 6 summarizes the work done in this paper.

All the mathematical notations used in this article are summarized in Table 1:

2. Distributed Detection of Signal under Chaotic Noise

In this paper, the distributed detection fusion system is used to detect weak signal under chaotic noise. This part is mainly divided into two aspects: one is the introduction of distributed detection fusion system, and the other is hypothesis testing of the observed signal of each local sensor under chaotic noise.

2.1. Distributed Detection Fusion System. The distributed detection fusion system is composed of a fusion center and multiple local sensors. In this paper, a distributed fusion system is considered with a parallel structure depicted in Figure 1, which has N local sensors and a fusion center.

As shown in Figure 1, the local sensors observe and judge the same target independently and transmit the results to the fusion center of the fusion system. Moreover, the fusion center fuses the received decision results of local sensors to obtain the final decision result.

2.2. Detection and Fusion of Weak Signal. Under the observation mechanism of the distributed system, the detection problem of the weak signal under chaotic noise can be divided into two parts in form. That is, the detection of the weak signal of local sensors and the fusion processing of local detection results by the fusion center.

2.2.1. Detection of Weak Signal by Local Sensors. Let the null hypothesis H_0 and alternative hypothesis H_1 are two hypotheses of prior probability P_0 and P_1, which represent the probability without and with signal, respectively. In this paper, the scenario is considered that the target is in a chaotic noise environment. Each sensor observes the same target. The observation signal of each sensor is composed of the same chaotic signal, the same target signal, and observation white noise of each sensor. For example, when using a sensor to monitor ships on the sea surface, the sea clutter can be approximated as chaotic noise. The observed signal of each sensor is a mixture of chaotic signal, target signal, and the white noise. The problem of detecting weak signal under chaotic noise by local sensors can be abstracted into the following hypothesis test problem:

$$\begin{aligned} H_0 &: y_k(t) = c(t) + n_k(t), \\ H_1 &: y_k(t) = c(t) + n_k(t) + s(t), \end{aligned} \tag{1}$$

where $k = 1, 2, 3, \cdots, N$. All local sensors observe the same target and the observation of the kth local sensor can be expressed as $y_k(t)$. $c(t)$ denote the background signal of chaotic noise from the interference of the environment of the phenomenon or target. The chaotic noise contained in the observation signal of each local sensor is the same. And $n_k(t)$ is the observed white noise of the kth local sensor, which obeys the normal distribution with a mean value of 0 and variance of σ_k^2. $s(t)$ denotes the target signal, namely, weak

Table 1: Mathematical notations and descriptions.

Mathematical notations	Description
H_0	The null hypothesis
H_1	The alternative hypothesis
P_0	The prior probability, which represents the probability without signal
P_1	The prior probability, which represents the probability with signal
$y_k(t)$	The observation of the kth local sensor at time t
$s(t)$	The target signal to be detected at time t
$c(t)$	The background signal of chaotic noise at time t
$n_k(t)$	The observed white noise of the kth local sensor at time t
σ_k^2	The variance of white noise
u_k	The decision result of the kth local sensor
$\boldsymbol{u}$	Decision vectors for all local sensors
u_0	The decision result of the fusion center
γ_k	The decision rule of the kth sensor
γ_0	The fusion rule of fusion center
g_k	A continued vector mapping
e_k	The fitting errors
δ	The threshold value for testing the model
τ	The time delays
m	The embedding dimensions
R_B	The Bayes risk of the detection fusion system
T_k	The decision threshold of the kth local sensor
P_D^k	The detection probability of the kth sensor
P_F^k	The false alarm probability of the kth sensor
P_D^0	The detection probability of fusion center
P_F^0	The false alarm probability of fusion center
C_{ij}	The cost of the global decision being H_j when H_j is present
$\tilde{u}_k$	The vector with the resulting decision of all local sensors except the kth sensor

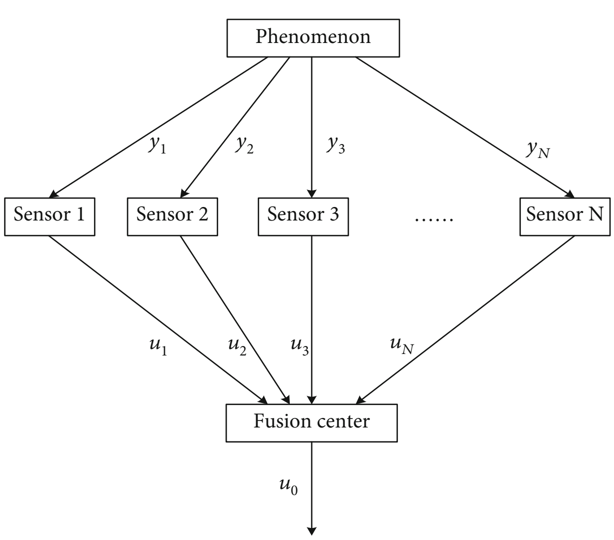

Figure 1: Distribution detection fusion system.

signal, which is independent of chaotic noise and is the signal of interest to us.

The weak signal to be detected is drowning under chaotic noise. If we use equation (1) to detect the signal directly, we should not be able to detect whether there is a weak signal $s(t)$ in the observed signal $y_k(t)$ accurately. It is necessary to eliminate the interference of chaotic noise $c(t)$. In other words, the chaotic signal can be fitted by using chaotic characteristics to eliminate the influence of chaotic noise. Thus, it is transformed into the following hypothesis testing problem:

$$\begin{aligned} H_0^* &: y_k(t) - c(t) = n_k(t), \\ H_1^* &: y_k(t) - c(t) = n_k(t) + s(t). \end{aligned} \tag{2}$$

The hypothesis test of local sensors in distributed detection fusion system under chaotic noise is proposed. It provides the hypothesis basis for the phase space reconstruction of the observation signal and the construction of the local weighted regression model in the next part.

2.2.2. Fusion of Local Detection Results. If the decision result of the kth local sensor is

$$u_k = \begin{cases} 0, H_0 \text{ is declared present}, \\ 1, H_1 \text{ is declared present}. \end{cases} \quad (3)$$

The observation result of all local sensors outputs is $\boldsymbol{u} = \{u_1, u_2, \cdots, u_N\}$. The decision of the fusion center is to fuse the decision of each local sensor and make the final decision, which can be expressed as u_0. While $u_0 = 1$ indicates the final decision result of fusion system is that there is a weak signal, $u_0 = 0$ indicates the final decision result of fusion system is no signal, i.e.,

$$u_0 = \begin{cases} 0, H_0 \text{ is declared present}, \\ 1, H_1 \text{ is declared present}. \end{cases} \quad (4)$$

Supposed the local sensors in the fusion system are independent of each other. The optimization goal of distributed fusion system is to seek a system decision rule in order to achieve the best performance of the fusion system:

$$\boldsymbol{\gamma} = \{\gamma_0, \gamma_1, \gamma_2, \cdots, \gamma_N\}, \quad (5)$$

where γ_k and γ_0 denote the fusion rule and decision rule at the kth sensor, respectively, which map from observation space to decision space as follows:

$$\begin{aligned} u_k &= \gamma_k(y_k), k = 1, 2, \cdots, N, \\ u_0 &= \gamma_0(\boldsymbol{u}) = \gamma_0(u_1, u_2, \cdots, u_N). \end{aligned} \quad (6)$$

3. Phase Space Reconstruction and LOWESS Model

The steps of establishing a single-step prediction model for the observed signals of the local sensor are as follows: step 1, reconstructing the phase space of observed signal; step 2, establishing the LOWESS model; step 3, testing the advantages and disadvantages of a local weighted regression model.

3.1. Phase Space Reconstruction. A phase space of m dimension can be constructed by the time delays τ and embedding dimensions m for the observed signal of k sensor $\{y_k(t), t = 1, 2, \cdots, n\}$. Any phase point in reconstructed phase space can be expressed as $Y_k(t) = (y_k(t), y_k(t-\tau), y_k(t-2\tau), \cdots, y_k(t-(m-1)\tau))'$, where $t = n_1, n_1 + 1, n_1 + 2, \cdots, n$ and $n_1 = 1 + (m-1)\tau$.

According to Takens delay embedding theorem [42], there is a continued vector mapping $g_k : R^m \longrightarrow R$ for every phase point of reconstructed phase space, that is, $y_k(t+1) = g(Y_k(t)), t = n_1, n_1 + 1, n_1 + 2, \cdots, n-1$. If the continuous vector mapping g_k or its approximation $\hat{g}_k$ can be obtained, the next data point $y_k(t+1)$ can be predicted according to the mapping. The time delays and embedding dimensions can be solved by the method of multiple autocorrelations [43] and Cao [44], respectively.

3.2. Locally Weighted Regression (LOWESS) Model. Local polynomial fitting is a widely used nonparametric technique, which combines the simplicity of traditional linear regression and the flexibility of nonlinear regression. It can eliminate the influence of heteroscedasticity and fit the data well, so we used the locally weighted regression model to predict. For the reconstructed phase space, the LOWESS model of the observed signal $y_k(t)$ is established to approximate the mapping g_k

$$\begin{aligned} &y_k(t+1) \approx g(Y_k(t)), \\ &g(Y_k(t)) = c_{0k} + c_{1k}^{(1)} y_k(t) + c_{2k}^{(1)} y_k(t-\tau) + \cdots + c_{mk}^{(1)} y_k(t-(m-1)\tau) + c_{1k}^{(2)} {y_k}^2(t) + \cdots + c_{mk}^{(s)} {y_k}^s(t-(m-1)\tau) = C_k' Y_k(t), \end{aligned} \quad (7)$$

where $C_k = (c_{0k}, c_{1k}^{(1)}, c_{2k}^{(1)}, \cdots, c_{mk}^{(1)}, c_{1k}^{(2)}, \cdots, c_{mk}^{(s)})'$. And C_k is the coefficient vector to be estimated in the original equation (7) and s is the order of the LOWESS model. For any phase point in phase space, there are some adjacent points around it with similar evolution law. The closer the distance is, the greater the degree of evolution similarity is. In this paper, the Euclidean distance of these phase points is calculated to determine these adjacent points. Suppose that a phase point $Y_k(t_M)$ is arbitrarily selected and there are q adjacent points $Y_k(t_i)(i = 1, 2, \cdots, q)$ around it, and $q \le 2m + 1$. The cubic function W is used to control the influence of the error caused by the point far away from the current point in the modeling process. The estimated value $\hat{C}_k$ of the parameter C_k is obtained by using the weighted-least-square method to solve the equation (7).

$$\min_{C_k \in R} \sum_{i=1}^{q} [y_k(t_i + 1) - g(Y_k(t_i))]^2 W(u_i) = \min_{C_k \in R} \sum_{i=1}^{q} \left[y_k(t_i + 1) - C_k' Y_k(t_i)\right]^2 W(u_i), \quad (8)$$

where

$$W(u_i) = \left(1\text{-}u_i^3\right)^3 \quad (i = 1, 2, \cdots, q),$$
$$u_i = \frac{d(Y_k(t_M), Y_k(t_i))}{\text{MAX}\left(d(Y_k(t_M), Y_k(t_i))\right)}, \tag{9}$$
$$W = \text{diag}\left(W(u_1), W(u_2), \cdots, W\left(u_q\right)\right),$$

$$Y_k = \begin{bmatrix} 1 & y_k(t_1) & y_k(t_1-\tau) & \cdots & y_k(t_1-(m-1)\tau) & {y_k}^2(t_1) & \cdots & {y_k}^s(t_1-(m-1)\tau) \\ 1 & y_k(t_2) & y_k(t_2-\tau) & \cdots & y_k(t_2-(m-1)\tau) & {y_k}^2(t_2) & \cdots & {y_k}^s(t_2-(m-1)\tau) \\ \vdots & \vdots & \vdots & \vdots & \vdots & \vdots & \vdots & \vdots \\ 1 & y_k\left(t_q\right) & y_k\left(t_q-\tau\right) & \cdots & y_k\left(t_q-(m-1)\tau\right) & {y_k}^2\left(t_q\right) & \cdots & {y_k}^s\left(t_q-(m-1)\tau\right) \end{bmatrix} = \begin{bmatrix} Y_k(t_1) \\ Y_k(t_2) \\ \vdots \\ Y_k\left(t_q\right) \end{bmatrix}, \tag{10}$$
$$\tilde{Y}_k = \left(y_k(t_1+1), y_k(t_2+1), \cdots, y_k\left(t_q+1\right)\right)'.$$

According to equation (8), the solution vector obtained by the local-weighted-least-square method is $\widehat{C}_k = \left(Y_k' W Y_k\right)^{-1} Y_k' W \tilde{Y}_k$. The predicted value $g(Y_k(t))$ can be obtained by substituting $\widehat{C}_k$ into the original equation, and the prediction error is $e_k(t+1) = y_k(t+1) - g\left(Y_k(t)\right)$.

3.3. Testing the Advantages and Disadvantages of LOWESS Model. Set a threshold value δ, when $m = 6$, $\tau = 7$ [21], $q = 4$, if the error sum of squares ($\text{sse} = \sum_{t=n_1}^{n-1} e_k^2(t+1)$) in LOWESS model is less than the threshold value δ, i.e., sse < δ (according to a large number of simulation results, let $\delta = 3$), then the LOWESS model can approximate the mapping g well; otherwise, it means that the LOWESS model cannot approximate the mapping g well and needs to be optimized again.

4. Detection Fusion Optimization Model and Its Solutions

This paper is aimed to construct a detection and fusion mechanism under chaotic noise based on the distributed detection system. It is mainly divided into two parts, one is to deal with chaotic signal, and the other is to detect and fuse the processed signal. The specific idea is shown in Figure 2.

The first part has been dealt with in the previous section, and followed by the second part, which is the distributed detection fusion of prediction errors. The problem of distributed detection fusion is to seek a set of optimal rules. Aiming at minimizing the Bayes risk of fusion center, a detection fusion optimization model is established. The optimization problem is a global optimization problem which involves the decision rules of local sensors and the fusion rule of fusion center. Because the chaotic noise has a great influence on the target signal, it cannot be solved when calculating the decision rules. Therefore, the chaotic noise has been stripped away before calculating the decision rules. In this paper, it is assumed that each local sensor is independent of each other, i.e., the observed signals of each sensor are conditionally independent of each other.

4.1. Detection Fusion Optimization Model. Since the chaotic noise has been stripped off in the previous part, the new observation of each local sensor is the fitting errors of the LOWESS model. A distributed detection fusion system is constructed according to the prediction error after stripping chaotic noise, as shown in Figure 3.

Let the conditional probability density function of the observed values e_k at the kth sensor is $f_{E_k}(e_k|\mathrm{H}_j)$, $j = 0, 1$ and $k = 1, 2, \cdots, N$. And the combined conditional probability density function of all local sensors is $f(e_1, e_2, \cdots, e_N|H_i)$, $i = 0, 1$. Assume that the local observations in the fusion system are conditional independence, namely the combined conditional probability density function is

$$f(e_1, e_2, \cdots, e_N|H_i) = \prod f(e_k|H_i), \tag{11}$$

Under the Bayesian criterion, denote the probabilities of detection and false at the kth sensor and fusion center by P_D^k, P_F^k, P_D^0, and P_F^0, respectively. The distributed detection fusion is modeled by minimizing the following Bayes risk:

$$R_B = \sum_{i=0}^{1}\sum_{j=0}^{1} C_{ij} P_j P\left(u_0 = i \middle| H_j\right), \tag{12}$$

where C_{ij} is the cost of the global decision being H_i when H_j is present.

As $P(u_0 = i|H_1) = (P_D^0)^i (1 - P_D^0)^{1-i}$, $P(u_0 = i|H_0) = (P_F^0)^i (1 - P_F^0)^{1-i}$,

$$
\begin{aligned}
R_B = \sum_{i=0}^{1}\sum_{j=0}^{1} C_{ij}P_jP\left(u_0 = i\middle|H_j\right) &= C_{00}P_0P(u_0 = 0|H_0) + C_{01}P_1P(u_0 = 0|H_1) \\
&+ C_{10}P_0P(u_0 = 1|H_0) + C_{11}P_1P(u_0 = 1|H_1) = C_{00}P_0\left(1 - P_F^0\right) + C_{01}P_1\left(1 - P_D^0\right) \\
&+ C_{10}P_0P_F^0 + C_{11}P_1P_D^0 = C_{00}P_0 - C_{00}P_0P_F^0 + C_{01}P_1 - C_{01}P_1P_D^0 + C_{10}P_0P_F^0 \\
&+ C_{11}P_1P_D^0 = (C_{10}P_1 + C_{00}P_0) + P_1(C_{01} - C_{11})P_F^0 - P_0(C_{10} - C_{00})P_F^0,
\end{aligned}
\tag{13}
$$

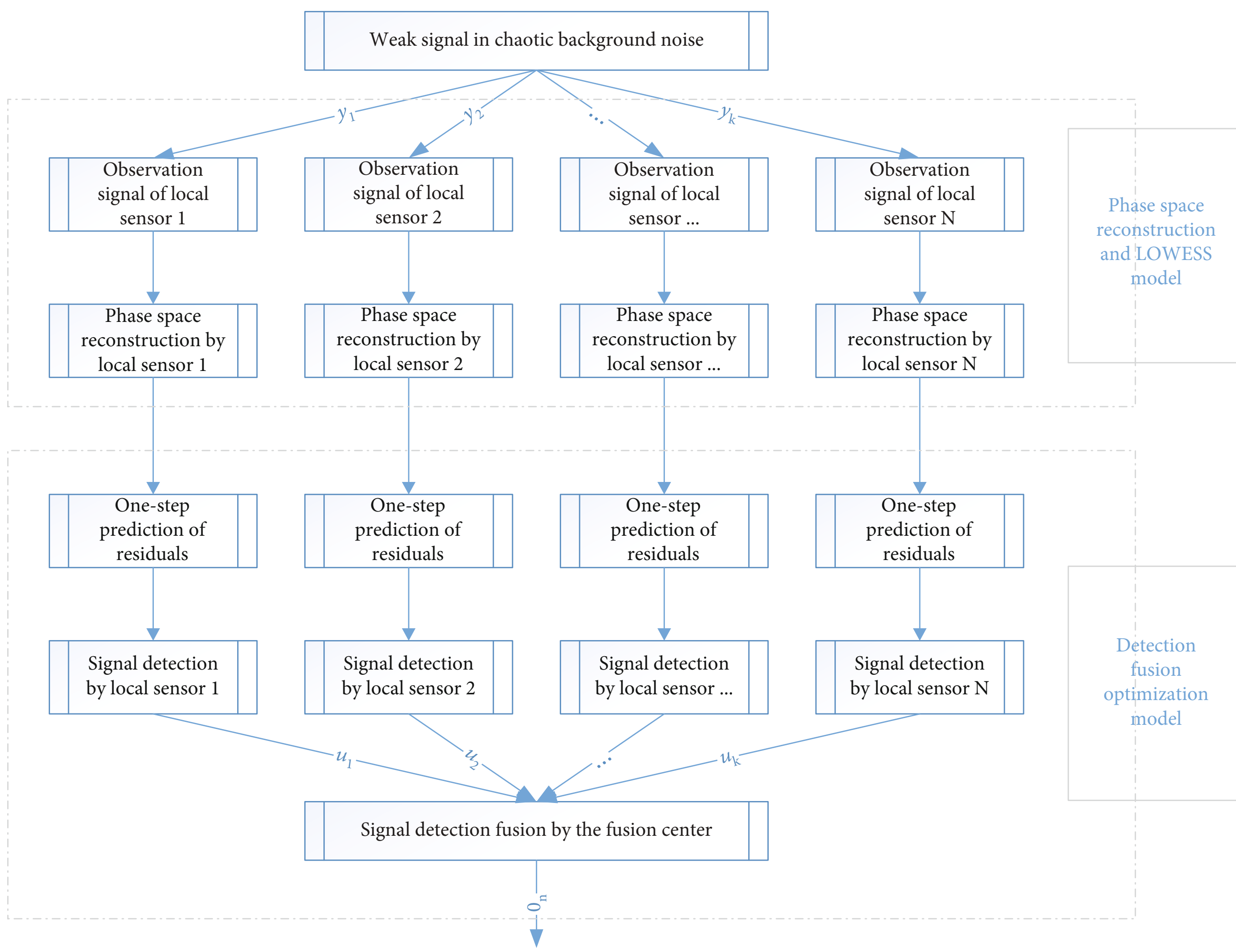

Figure 2: Schematic diagram of detection fusion of weak signal under chaotic noise.

and then

$$
R_B = C + C_F P_F^0 - C_D P_D^0, \tag{14}
$$

where $C = C_{10}P_1 + C_{00}P_0, C_F = P_1(C_{01} - C_{11})$, $C_D = P_0(C_{10} - C_{00})$.

Because $P_D^0 = P(u_0 = 1|H_1), P_F^0 = P(u_0 = 1|H_0)$, then

$$
\begin{aligned}
P_F^0 &= \sum_{\boldsymbol{u}} P(u_0 = 1|\boldsymbol{u})P(\boldsymbol{u}|H_0), \\
P_D^0 &= \sum_{\boldsymbol{u}} P(u_0 = 1|\boldsymbol{u})P(\boldsymbol{u}|H_1).
\end{aligned}
\tag{15}
$$

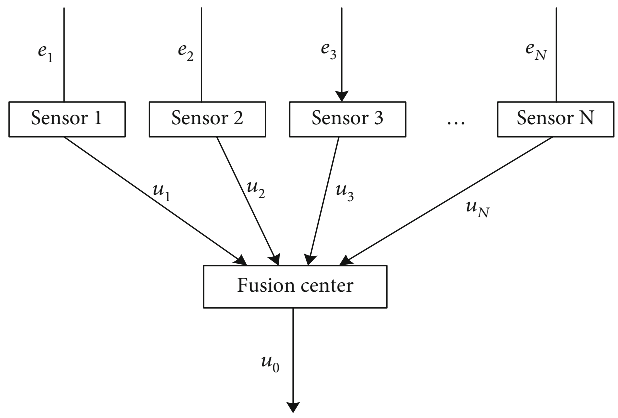

Figure 3: The distributed detection fusion system of fitting errors.

Thus, the Bayes risk function can be expressed as

$$R_B = C + \sum_{\boldsymbol{u}} P(u_0 = 1|\boldsymbol{u})[C_F P(\boldsymbol{u}|H_0) - C_D P(\boldsymbol{u}|H_1)]. \quad (16)$$

According to formula (10), the Bayes risk function is determined by the decision rules of each local sensor and the fusion rule of the fusion center. Therefore, it is necessary to seek the optimal fusion rule for the whole system and optimal sensor decision rules by minimizing the Bayes risk of fusion system, i.e.,

$$\min R_B = C + \sum_{\boldsymbol{u}} P(u_0 = 1|\boldsymbol{u})[C_F P(\boldsymbol{u}|H_0) - C_D P(\boldsymbol{u}|H_1)]. \quad (17)$$

Although the above model is relatively simple in form, the decision rules of local sensors and the fusion rule are complex in form. As they were coupled together, the model may be difficult to solve. The idea of Gauss Seidel's algorithm is used to solve the rules. The conditional probability density function can be obtained by fitting the distribution of prediction errors by parameter estimation.

4.2. Fusion Rule and Decision Rules of Local Sensors. The fusion rule and decision rules of the local sensor are obtained by the detection fusion optimization model. If the decision rules of local sensors were known, we could find out the optimal fusion rule to when the Bayes risk reaches the minimum. If the fusion rule of the fusion center and the other decision rules of local sensors were known, we could also find out the optimal decision rule of the kth local sensor to minimizing the Bayesian risk. The optimal fusion rule and decision rules of local sensors can be obtained by solving the two rules jointly.

4.2.1. Fusion Rule. Suppose that the decision rules of local sensors were known, i.e., $P(\boldsymbol{u}|H_i), i = 0, 1$. If the Bayes risk function of the fusion system was to be minimized, the conditional probability needed to satisfy

$$P(u_0 = 1|\boldsymbol{u}) = \begin{cases} 1, & \text{if } \dfrac{C_F P(\boldsymbol{u}|H_0)}{C_D P(\boldsymbol{u}|H_1)} < 1, \\ 0, & \text{otherwise.} \end{cases} \quad (18)$$

Then, the optimal fusion rule of the fusion center is expressed as

$$\frac{P(\boldsymbol{u}|H_1)}{P(\boldsymbol{u}|H_0)} \underset{H_0}{\overset{H_1}{\gtrless}} \frac{C_F}{C_D}. \quad (19)$$

4.2.2. Local Sensor Decision Rule. Suppose that the fusion rule of fusion center was $P(u_0 = 1|\boldsymbol{u})$. If the other decision rules of local sensors were known, the decision rule at the kth sensor could be found when the Bayes risk reach the minimum. Denote the resulting decision of all local sensors except the kth sensor by $\tilde{u}_k = (u_1, u_1, \cdots, u_{k-1}, u_{k+1}, \cdots, u_N)$. The probabilities of detection and false in the fusion system can expressed as

$$\begin{aligned} P_D^0 &= \sum_{\tilde{u}_k} \{P(u_0 = 1|\tilde{u}_k, u_k = 0)P(\tilde{u}_k, u_k = 0|H_1) + P(u_0 = 1|\tilde{u}_k, u_k = 1)P(\tilde{u}_k, u_k = 1|H_1)\}, \\ P_F^0 &= \sum_{\tilde{u}_k} P(u_0 = 1|\tilde{u}_k, u_k = 0)P(\tilde{u}_k|H_0) + \sum_{\tilde{u}_k} A(\tilde{u}_k)P(\tilde{u}_k, u_k = 1|H_0) \\ &= \sum_{\tilde{u}_k} \{P(u_0 = 1|\tilde{u}_k, u_k = 0)(P(\tilde{u}_k|H_1) - P(\tilde{u}_k, u_k = 1|H_1)) + P(u_0 = 1|\tilde{u}_k, u_k = 1) \cdot P(\tilde{u}_k, u_k = 1|H_1)\} \\ &= \sum_{\tilde{u}_k} P(u_0 = 1|\tilde{u}_k, u_k = 0)P(\tilde{u}_k|H_1) + \sum_{\tilde{u}_k} A(\tilde{u}_k)P(\tilde{u}_k, u_k = 1|H_1). \end{aligned} \quad (20)$$

Then, the Bayes risk function can be expressed as

$$R_B = C_k + C_F \sum_{\tilde{u}_k} A(\tilde{u}_k) P(\tilde{u}_k, u_k = 1|H_0) - C_D \sum_{\tilde{u}_k} A(\tilde{u}_k) P(\tilde{u}_k, u_k = 1|H_1), \tag{21}$$

where

$$\begin{aligned} A(\tilde{u}_k) &= P(u_0 = 1|\tilde{u}_k, u_k = 1) - P(u_0 = 1|\tilde{u}_k, u_k = 0), \\ C_k &= C + \sum_{\tilde{u}_k} P(u_0 = 1|\tilde{u}_k, u_k = 0)\{C_F P(\tilde{u}_k|H_0) - C_D P(\tilde{u}_k|H_1)\}. \end{aligned} \tag{22}$$

The Bayes risk function of the fusion system is

$$\begin{aligned} R_B = C_k + \int_{e_k} P(u_k = 1|e_k) \Big\{ & C_F \sum_{\tilde{u}_k} A(\tilde{u}_k) P(\tilde{u}_k|H_0) \cdot f_{E_k}(e_k|H_0) \\ & - C_D \sum_{\tilde{u}_k} A(\tilde{u}_k) P(\tilde{u}_k|H_1) f_{E_k}(e_k|H_1) \Big\} de_k. \end{aligned} \tag{23}$$

If the Bayes risk function of the fusion system was to be minimized, then

$$u_k = \begin{cases} 1, & \text{if } \dfrac{C_F \sum_{\tilde{u}_k} A(\tilde{u}_k) P(\tilde{u}_k|H_0)}{C_D \sum_{\tilde{u}_k} A(\tilde{u}_k) P(\tilde{u}_k|H_1)} < \dfrac{f_{E_k}(e_k|H_1)}{f_{E_k}(e_k|H_0)}. \\ 0, & otherwise. \end{cases} \tag{24}$$

The optimal decision rule at the kth sensor is expressed as

$$\frac{f_{E_k}(e_k \mid H_1)}{f_{E_k}(e_k \mid H_0)} \underset{H_0}{\overset{H_1}{\gtrless}} \frac{C_F \sum_{\tilde{u}_k} A(\tilde{u}_k) P(\tilde{u}_k \mid H_0)}{C_D \sum_{\tilde{u}_k} A(\tilde{u}_k) P(\tilde{u}_k \mid H_1)}. \tag{25}$$

Let the kth local sensor decision threshold is

$$T_k = \frac{C_F \sum_{\tilde{u}_k} A(\tilde{u}_k) P(\tilde{u}_k|H_0)}{C_D \sum_{\tilde{u}_k} A(\tilde{u}_k) P(\tilde{u}_k|H_1)}. \tag{26}$$

Therefore, there are N optimal decision rule equations and 2^N fusion equations. According to formula (13), the optimal fusion rule under the condition each local sensor is independent of each other is expressed as

$$\prod_{i=1}^{N} \frac{P(u_i|H_1)}{P(u_i|H_0)} \underset{H_0}{\overset{H_1}{\gtrless}} \frac{C_F}{C_D}. \tag{27}$$

The fusion rule and the decision rules of local sensors are coupled with each other. In order to obtain the optimal decision rule of the whole system, it is necessary to solve the optimal decision thresholds of every local sensor and optimal fusion rule of the fusion center.

4.2.3. Iterative Algorithm. According to the content of the upper part, the optimal decision rules can be simplified as a likelihood ratio threshold decision under the condition of independent observation of each local sensor. In other words, the optimal rules of the fusion system can be obtained directly from the optimal fusion rule and local sensor decision thresholds. The decision rules of local sensors and the fusion rule of fusion center are coupled together, and the model may be difficult to solve. The idea of Gauss Seidel's algorithm is used to solve the rules. The fusion rule and the corresponding set of local sensor decision thresholds that yield the minimum cost constitute the solution of the hypothesis testing problem in distributed detection fusion system. The numerical iterative algorithm is initialized by picking a set of local sensor decision thresholds and fusion rule. The optimal fusion rule and local sensor decision thresholds are obtained by minimizing the Bayes risk, respectively. Once the first iteration is complete, the next iterations are run identically. The numerical iteration algorithm is terminated when the difference of Bayes risks obtained after two successive iterations is less than the given accuracy.

Its pseudocodes are as follows:

Inputs: Prediction errors $e_k(t)$;
Outputs: The optimal fusion rule γ_0 and the optimal sensor decision threshold T_k;
Begin:
Initialization parameters: γ_0^0, T_k^0, $(k = 1, 2, \cdots, N)$ etc;
Termination criteria: $while(R_B^{n+1} - R_B^n > \varepsilon)$
Step 1: According to the initial values $\{\gamma_0^0, T_1^0, T_2^0, \cdots, T_N^0\}$, calculate their corresponding Bayes risk value R_B^0;
Step 2: Fixed $\{T_1^{n-1}, T_2^{n-1}, \cdots, T_N^{n-1}\}$, calculate the optimal fusion rule γ_0^n;
Step 3: For the first sensor, fix $\{\gamma_0^n, T_2^n, \cdots, T_{k-1}^n, T_{k+1}^{n-1}, \cdots, T_N^{n-1}\}$ and calculate the decision threshold T_1^n. Similarly, for the kth sensor, $\{\gamma_0^n, T_1^n, \cdots, T_{k-1}^n, T_{k+1}^{n-1}, \cdots, T_N^{n-1}\}$is fixed and calculate the decision threshold T_k^n;
Step 4: According to the fusion rule γ_0^n and decision threshold $\{T_1^n, T_2^n, \cdots, T_N^n\}$, calculate the Bayes risk value R_B^n;
Step 5: If R_B^n does not satisfied the for a given precision, then let $n = n + 1$ and turn step 2 to continue the cycle, otherwise stop the cycle and output the optimal fusion rule and sensor decision threshold $\{\gamma_0^n, T_1^n, T_2^n, \cdots, T_N^n\}$.
End while

Pseudocode 1:

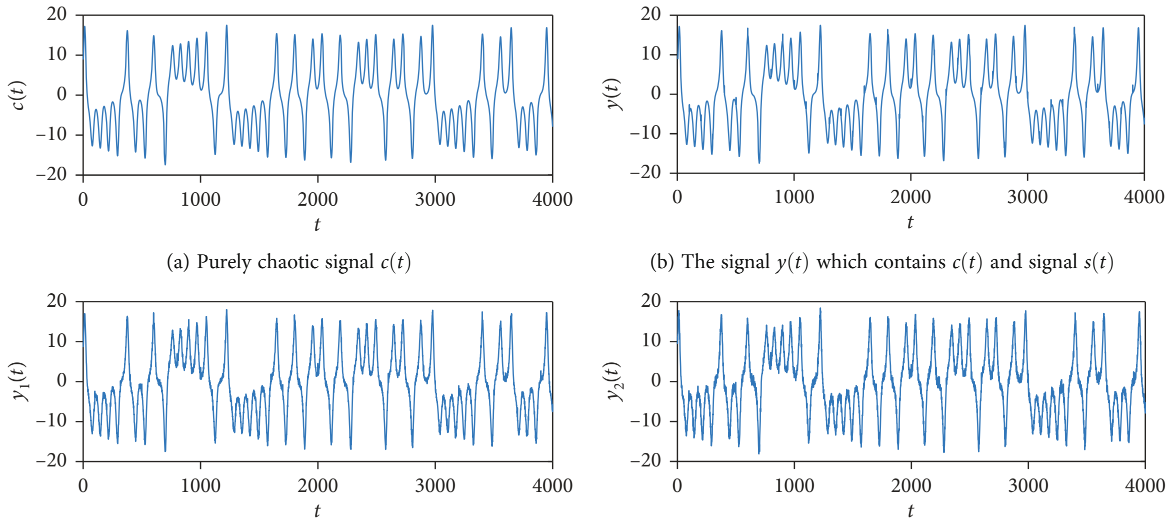

(a) Purely chaotic signal $c(t)$

(b) The signal $y(t)$ which contains $c(t)$ and signal $s(t)$

(c) The observation signal $y_1(t)$ is combined with the true signal, chaotic signal, and observed white noise from the DM1

(d) The observation signal $y_2(t)$ is combined with the true signal, chaotic signal, and observed white noise from the DM2

Figure 4: The results of signals.

5. Simulations

In this paper, the binary hypothesis testing problem for a parallel distributed detection fusion system with two local sensors is simulated. The local sensors are independent of each other, which are named as DM1 and DM2, respectively. For convenience, suppose that all local sensor has the same performance.

In order to verify the feasibility and effectiveness of the proposed method, four simulation experiments were carried out. A Lorenz system is used to generate the chaotic signals based on the literature [20, 21], and the white noise in the observation signal of the kth sensor obeys the normal distribution with a mean value of 0, i.e., $n_k(t) \sim N(0, \sigma_k^2), k = 1, 2$. The signal-to-noise ratio (SNR) is used to measure the detection threshold.

$$SNR = 10\lg\left(\frac{\sigma_s^2}{\sigma_c^2 + \sigma_n^2}\right), \tag{28}$$

where

$$\begin{aligned} \sigma_s^2 &= \frac{1}{n}\sum_{t=1}^{n}\left(s(t) - \bar{s}(t)\right)^2, \\ \sigma_c^2 &= \frac{1}{n}\sum_{t=1}^{n}\left(c(t) - \bar{c}(t)\right)^2. \end{aligned} \tag{29}$$

$\bar{s}(t)$ and $\bar{c}(t)$ are the means of $s(t)$ and $c(t)$, respectively, σ_c^2 and σ_s^2 are the variance of the chaotic signal and the target signal, respectively. σ_n^2 is the maximum of the variance of white noise $n_k(t)$. The chaotic signal is stronger compared to the target signal. The target signal is almost drowned out by the chaotic signal, resulting in a low SNR. In this paper, the chaotic signal is stripped before local sensors detect and fuse the observation signals.

Consider Lorenz system

$$\begin{cases} \dot{x} = \sigma(y - x), \\ \dot{y} = -xz + rx - y, \\ \dot{z} = xy - bz, \end{cases} \tag{30}$$

where $\sigma = 10, b = 8/3, r = 28, x, y, z$ denote the time function. The initial points are $x = 1, y = 1, z = 1$ and the step length of the integral is $t = 0.01s$. We apply a four-order *Runge-Kutta* integral method and obtain a simulated time series of x with 10000 data. To reduce the influence of transition, we get rid of the first and the last 3000 data and only keep the middle 4000 data, i.e., $\{c(t), t = 1, 2, 3, \cdots, 4000\}$. For the sequence of 4000 time points, we apply the method of multiple autocorrelation and Cao to obtain the time delay $\tau = 7$ and the embedding dimension $m = 6$ of observed signals, respectively.

5.1. Detection Experiment of Weak Signal Existence in Distributed Detection System. In this paper, the pulse signal is used as the target signal to be detected. Suppose that the signal is a pulse signal with a period of 100, i.e., $s(t) = p \cdot s_1(t)$, where $p = 2$

$$s_1(t) = \begin{cases} 1, & t = 100, 200, \cdots, \\ 0, & \text{others}, \end{cases} \tag{31}$$

producing a time series of 4000 and make it as $\{s(t), t = 1, 2, 3, \cdots, 4000\}$. Two local sensors observe the same phenomenon. Each local sensor itself has a certain observation error. This paper assumes that the variance of the local sensors observation error is 0.4 and 0.6, respectively. At this time, the SNR of two local sensors is -73.69 dB and -73.73 dB.

In this paper, two local sensors are used to observe the same phenomenon, and the observation signals are shown in Figure 4. Figures 4(a) and 4(b) show the purely chaotic

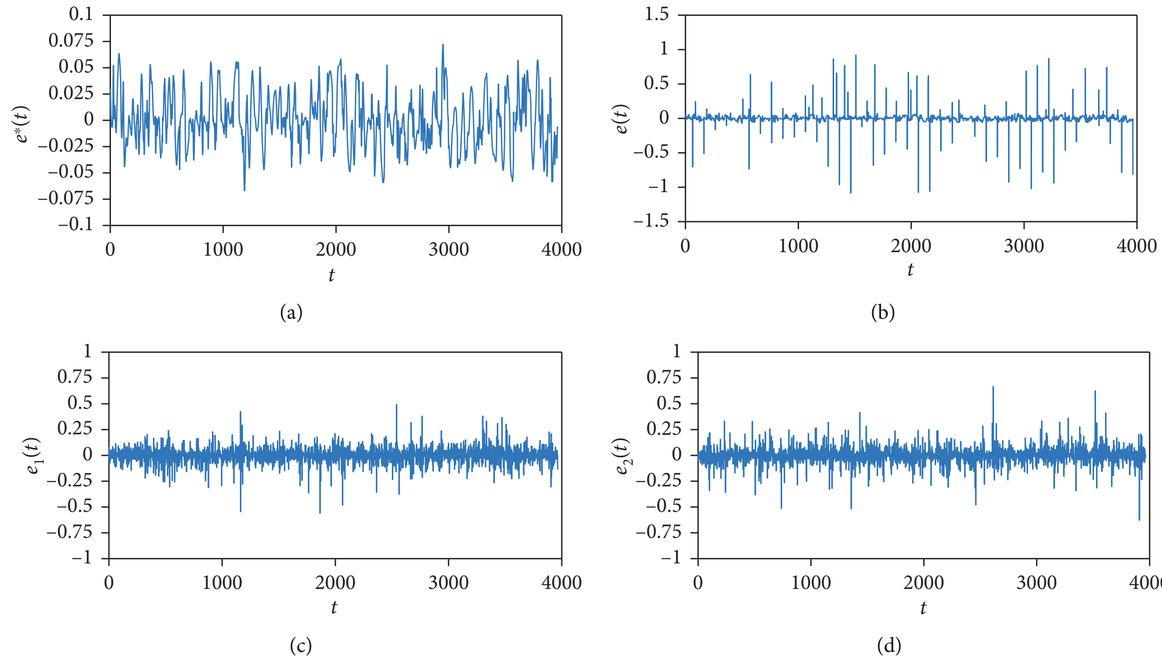

Figure 5: The fitting errors of signals. (a) Fitting error of $c(t)$. (b) Fitting error of $y(t)$. (c) Fitting error of $y_1(t)$. (d) Fitting error of $y_2(t)$.

Table 2: Evaluation index of different models.

Index	UR	LAR	LOWESS
MSE	0.1858	0.1072	0.0033
RMSE	0.4311	0.3274	0.0578
MAD	0.2168	0.1232	0.0365

signal $c(t)$ and the signal $y(t)$ which contain $c(t)$ and signal $s(t)$, respectively. Figures 4(c) and 4(d) show the observation signal $y_1(t)$ of DM1 and the observation signal $y_2(t)$ of DM2, respectively. The observation signal $y_i(t)$ is combined with the true signal, chaotic signal, and observed white noise from the DMi, $i = 1, 2$.

Figure 4 shows that the four signals are very similar. It is hard to differentiate directly. It seems that the influence of weak pulse signal on chaotic noise is very weak and has been submerged in chaotic noise. So the weak pulse signal cannot be detected directly.

Because the weak pulse signal has a weak impact on the chaotic signal, the delay times and embedding dimension of these signals obtained by the same method should be the same. In this paper, the phase space reconstruction is used to establish a local weighted regression model for $c(t)$, $y(t)$, $y_1(t)$, and $y_2(t)$, respectively, which can peel off the chaotic noise signal and obtain the corresponding fitting errors. These fitting errors are shown in Figure 5.

In Figure 5, $e^*(t)$, $e(t)$, $e_1(t)$, and $e_2(t)$ denote the fitting errors of $c(t)$, $y(t)$, $y_1(t)$, and $y_2(t)$, respectively. Phase space reconstruction and the LOWESS model can effectively divest the chaotic noise signal. The fitting errors increase obviously by stripping the chaotic noise, which means that there may be weak pulse signal in the observation signals. If the observation just contains pulse signal and chaotic noise, we could directly see whether there is a pulse signal from the fitting error. However, if the observation contains pulse signal, chaotic noise, and the white noise from local sensors, it was hard to judge the pulse signal directly. The detection fusion strategy would get more accurate results.

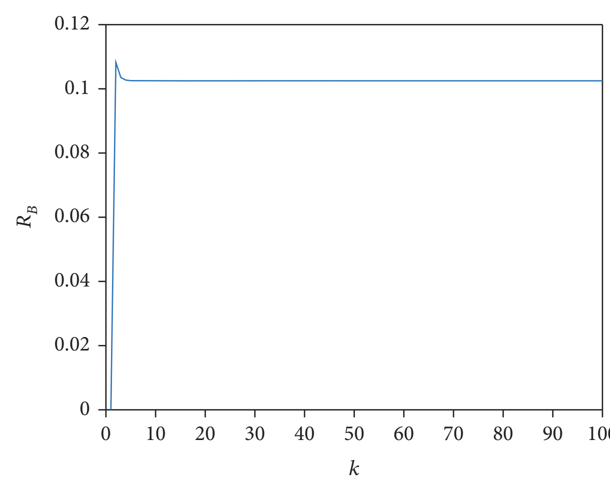

Figure 6: Iterative convergence result of fusion algorithm.

5.2. Performance Evaluation of LOWESS Model. In order to verify the performance of forecasting precision from the LOWESS model and demonstrate the advantages of this model, the three evaluation indexes of mean square error (MSE), mean absolute deviation (MAD), and root mean square error (RMSE) are used to measure performance.

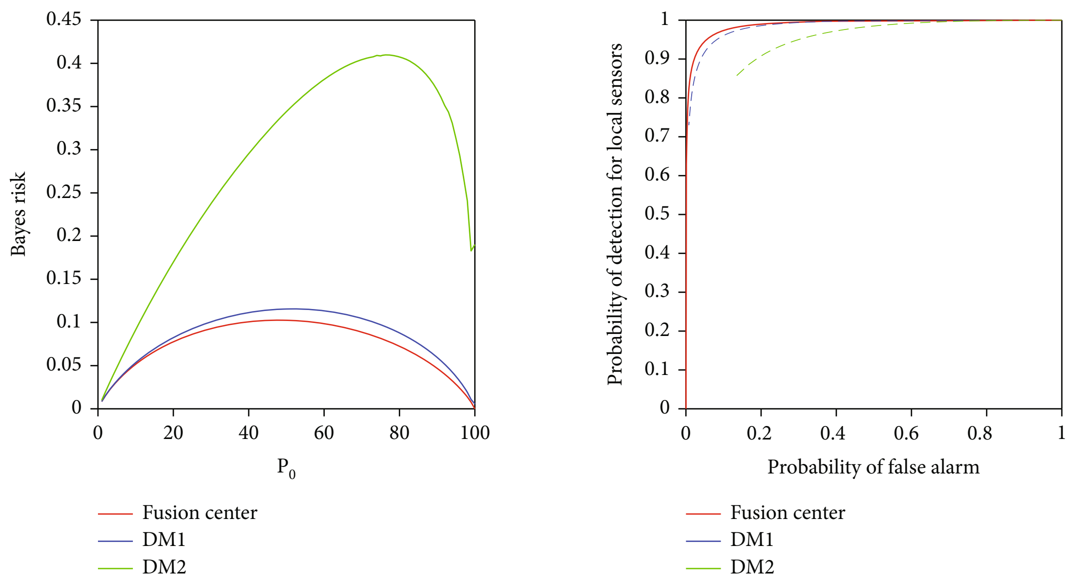

(a) The Bayes risk of fusion system with two local sensors DM1 and DM2

(b) The probability of false alarm and detection of fusion system with two sensors DM1 and DM2

Figure 7: The results of Bayes risks and detection performance.

Suppose the true value is $y(t)$ and the predicted value is $\hat{y}(t)$, then

$$\text{MSE} = \frac{1}{n}\sum_{t=1}^{n}(y(t) - y\wedge(t))^2,$$

$$\text{MAD} = \frac{1}{n}\sum_{t=1}^{n}|y(t) - \hat{y}(t)|, \quad (32)$$

$$\text{RMSE} = \sqrt{\frac{1}{n}\sum_{t=1}^{n}(y(t) - y\wedge(t))^2},$$

where n denotes the number of signal. $y(t)$ denotes the signal which is combined with the true and chaotic signal, i.e.,

$$y(t) = c(t) + s(t). \quad (33)$$

We compare the unreconstructed model (UR) and the linear model (LAR) with the locally weighted regression model (LOWESS) in this paper under the same experimental conditions, and the results are shown in Table 2.

In Table 2, it seems that the prediction effects of the reconstructed models are better than the unreconstructed model. That is because the reconstructed models can restore the dynamic system of chaos well. The prediction effect of the LOWESS model is better than the linear model. In addition, the linear model may be affected by outliers, which leads to large prediction error. The result of evaluation indexes from Table 2 is shown that the performance of LOWESS in this paper is better than the other two models.

5.3. Detection of Convergence Algorithm and Performance Evaluation. Aim to better illustrate the astringency and advantages of detection fusion algorithm, we also show the iterative convergence graph of the fusion algorithm and Bayes risk of single sensor and fusion system with two local sensors. When P_0 is equal to 0.5, the iterative convergence result is shown in Figure 6.

The value of Bayes risk (R_B) gradually tends to a fixed value when the number of iterations k increases. When k is greater than 5, the Bayes risk does not change, which shows

Table 3: Detection accuracy of different methods.

P_0	SNR/dB	DM 1	DM 2	Fusion center
0.9	-10	0.848	0.529	0.893
	-40	0.865	0.487	0.892
	-70	0.844	0.431	0.870
	-100	0.836	0.431	0.864
0.7	-10	0.664	0.479	0.682
	-40	0.669	0.458	0.681
	-70	0.641	0.434	0.657
	-100	0.639	0.444	0.663
0.5	-10	0.502	0.501	0.501
	-40	0.503	0.497	0.499
	-70	0.502	0.505	0.502
	-100	0.504	0.501	0.498
0.3	-10	0.662	0.690	0.715
	-40	0.662	0.685	0.701
	-70	0.646	0.667	0.693
	-100	0.635	0.667	0.695
0.1	-10	0.667	0.820	0.896
	-40	0.697	0.831	0.892
	-70	0.661	0.796	0.868
	-100	0.637	0.800	0.868

that the iterative has converged, at the same time, the Bayes risk value is 0.1025. This shows that the fusion algorithm has good convergence.

According to the optimal rules, the Bayes risks of each local sensor and fusion center in the fusion system are calculated. The corresponding probability of detection and false alarm are also calculated. The Bayes risks of fusion center and single local sensor are shown in Figure 7. Figure 7(a) shows the Bayes risks of the fusion system with two local sensors DM1 and DM2, and Figure 7(b) shows the detection performance of the local sensor and fusion center in the fusion system. The detection performance is represented by the probability of detection and false alarm.

According to Figure 7, the local sensors cooperate with each other, which can minimize the Bayes risk value. The fusion center result is better than the local sensor results. This fully demonstrates the superiority of distributed detection fusion system.

5.4. Comparison of Detection Fusion Results in Different Scenarios. In order to further illustrate the advantages of distributed detection fusion system under chaotic noise, its performance is analyzed under different parameter values. The results are shown in Table 3.

From Table 3, the results showed that the accuracy of the fusion system is generally higher than that of the single local sensor in different scenarios, and the partial performance of a single local sensor may be sacrificed owing to the coupling of optimal fusion algorithms, which leads to abnormal detection results of local sensors. The farther the P_0 value is from 0.5, the more superiority is. When the P_0 is close to 0.5, the superiority is not obvious, even the detection result of the fusion system is worse than that of single local sensor. Taken as a whole, the distributed detection fusion system has consistent advantages compared with single local sensor observation mechanism.

The precision (P), recall (R), accuracy (ACC), and comprehensive evaluation index (F_1) are used to evaluate the detection performance of fusion system:

$$P = \frac{TP}{TP + FP}, R = \frac{TP}{TP + FN}, F_1 = \frac{2 \times P \times R}{P + R}, \quad ACC = \frac{TP + TN}{TP + FP + FN + TN}, \tag{34}$$

where TP means that there is a signal in practice and is judged to be a signal; FP means that there is actually no signal, but the judgment is a signal; TN means that there is actually no signal and is judged to be no signal; FN means that there is a signal in practice, but the judgment is no signal.

Select the optimal result of the fusion system to set the parameters, that is, SNR = −51 dB and $P_0 = 0.1$, and the experimental results are shown in Tables 4 and 5.

From the results shown in Tables 4 and 5, in different scenarios, the detection performance of the fusion system is different. When SNR is equal to -51 dB, the detection performance of the fusion system increases with the decrease of the P_0 value. When P_0 is equal to 0.1, the detection performance of fusion system decreases with the decrease of SNR.

Table 4: Detection performance of different P_0 at SNR = −51 dB.

P_0	ACC	P	R	F_1
0.9	0.883	0.360	0.217	0.271
0.8	0.776	0.406	0.260	0.317
0.7	0.685	0.438	0.172	0.247
0.6	0.596	0.479	0.130	0.205
0.5	0.499	0.499	0.988	0.663
0.4	0.597	0.601	0.982	0.745
0.3	0.702	0.705	0.988	0.823
0.2	0.798	0.809	0.979	0.886
0.1	0.879	0.915	0.955	0.934

Table 5: Detection performance of different SNR at $P_0 = 0.1$.

SNR/dB	ACC	P	R	F_1
-10	0.896	0.975	0.907	0.940
-40	0.892	0.927	0.954	0.940
-70	0.868	0.903	0.955	0.929
-100	0.868	0.900	0.959	0.928
-150	0.860	0.899	0.951	0.924

5.5. Comparison of ROC Curves of Single Sensor and Fusion Center. In order to demonstrate the superiority of the proposed method, other detection fusion methods are compared with the proposed method. ROC curve is a curve drawn according to a series of different dichotomy methods (boundary value or decision threshold), with sensitivity (true positive rate, TPR) as vertical coordinate and 1-specificity (false positive rate, FPR) as horizontal coordinate, which is used to judge the detection results. The larger the area (AUC) under the ROC curve, the higher the accuracy of the detection results.

Figure 8 shows that the ROC curves of a single sensor (sensor 1 and sensor 2) and the fusion center of distributed detection fusion system are obtained when the SNR is -10 dB. From the results in Figure 8, the AUC value of the fusion center is 0.974, and it is greater than that of a single sensor, which indicates that the detection results of distributed detection fusion system have higher accuracy than that of a single sensor.

5.6. Comparison of Results of Different Detection Fusion Methods. In order to demonstrate the superiority of the proposed method, other detection fusion methods are compared with the proposed method. The prediction and fusion of the linear model and the unreconstructed model of the distributed sensor, namely, DS-LAR and DS-UR, are carried out, respectively, and compared with the proposed method in this paper. The detection fusion results of different models are shown in Table 6.

It can be seen from Table 6 that the detection and fusion results were obtained by using different methods when the

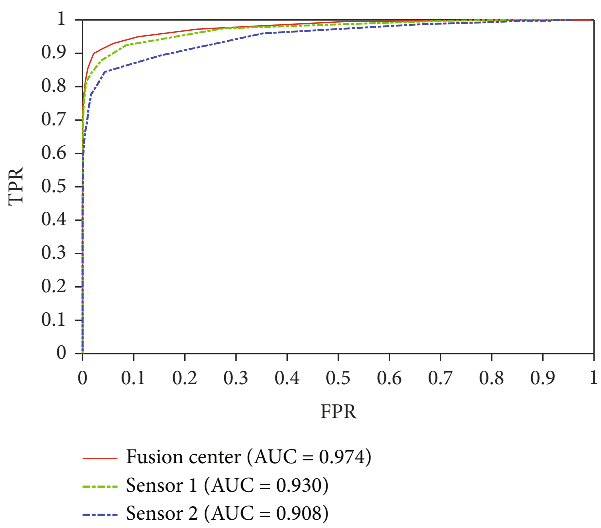

FIGURE 8: ROC curves of local sensors and fusion center.

TABLE 6: Detection and fusion results of different models at SNR = −10 dB.

Model	ACC	P	R	F_1
Proposed method	0.896	0.975	0.907	0.940
DS-LAR	0.855	0.988	0.849	0.913
DS-UR	0.656	0.997	0.619	0.764

SNR is -10 dB, and the proposed method in this paper has the highest detection accuracy. Although the precision of the proposed method is lower than that of DS-LAR and DS-UR, the comprehensive evaluation index (F_1) is higher. Therefore, the detection performance of the proposed method is better than the other two methods.

6. Conclusions

In this paper, the problem of signal detection under chaotic noise was considered in the distributed detection fusion system. In this paper, the problem of signal detection under chaotic noise was considered in the distributed detection fusion system. The problem which is urgent and difficult has important research value. And the related research is little. The signal detection theory under the background of chaotic noise is combined with the traditional distributed detection fusion theory. The proposed signal processing method and detection fusion algorithm could detect the target signal effectively, which means important theoretical significance and practical value. From the simulation results, we can draw the following conclusions: the LOWESS model could effectively remove chaotic noise; the proposed distributed fusion algorithm could converge rapidly; the results of detection fusion is obviously better than that of a single sensor; weak signals submerged in chaotic noise and white noise could be detected effectively; the proposed method was better than DS-LAR and DS-UR, and its detection accuracy is higher.

Data Availability

The process of generating experimental data has been given in this paper. In other words, the data used to support the findings of this study are included within the article.

Conflicts of Interest

The authors declare that they have no conflicts of interest.

Acknowledgments

This work was supported by the Chongqing Natural Science Foundation of China (Grant no. cstc2018jcyjAX0464, cstc2019jcyj-msxmX0491) and Chongqing postgraduate research and innovation project funding (Project No.: clgycx 20203143).

References

[1] Z. Cai, *Research on Weak Signal Detection and Processing in the Background of Strong Noise*, Inner Mongolia University of Science and Technology, Baotou, China, 2014.

[2] C. Nie and Y. Shi, “The reaserch of weak signal detection based on cross-orrelation and chaos theory,” *Chinese Journal of Scientific Instrument*, vol. 22, no. 1, pp. 32–35, 2001.

[3] K. Zhang and H. Zhu, “Weak signal detecting technology,” *Avionics Technology*, vol. 40, no. 2, 2009.

[4] H. Lv, Z. Cao, X. Yan, and P. Li, “A combined method of weak signal detection,” in *Proceedings of the Asia-Pacific Conference on Computational Intelligence and Industrial Applications*, pp. 106–109, Wuhan, China, 2009.

[5] Y. Li and B. Yang, “Chaotic system for the detection of periodic signals under the background of strong noise,” *Chinese Science Bulletin*, vol. 48, no. 5, pp. 508–510, 2003.

[6] H. Zheng, *Chaotic Synchronization and Its Application in Radar*, University of Electronic Science and Technology, Chengdu, China, 2011.

[7] J. He, Z. Liu, and S. Hu, “Detection of weak signal based on the sea clutter scattering,” *Acta Physica Sinica*, vol. 60, no. 11, 2011.

[8] Xing Hong-Yan, Zhu Qing-Qing, and Xu Wei, “A method of weak target detection based on the sea clutter,” *Acta Physica Sinica*, vol. 63, no. 10, p. 100505, 2014.

[9] H. Leung and S. Haykin, “Is there a radar clutter attractor?,” *Applied Physics Letters*, vol. 56, no. 6, pp. 593–595, 1990.

[10] H. Leung and T. Lo, “Chaotic radar signal processing over the sea,” *IEEE Journal of Oceanic Engineering*, vol. 18, no. 3, pp. 287–295, 1993.

[11] S. Haykin and Xiao Bo Li, “Detection of signals in chaos,” *Proceedings of the IEEE*, vol. 83, no. 1, pp. 95–122, 1995.

[12] H. Leung and Xinping Huang, “Parameter estimation in chaotic noise,” *IEEE Transactions on Signal Processing*, vol. 44, no. 10, pp. 2456–2463, 1996.

[13] S. Haykin and J. Principe, “Making sense of a complex world [chaotic events modeling],” *IEEE Signal Processing Magazine*, vol. 15, no. 3, pp. 66–81, 1998.

[14] Xing Hong-Yan, Zhang Qiang, and Xu Wei, “Hybrid algorithm for weak signal detection in chaotic sea clutter,” *Acta Physica Sinica*, vol. 64, no. 4, p. 040506, 2015.

[15] H. Xing, H. Wu, and G. Liu, "Variable-scale Duffing oscillator method for weak signal detection," *Acta Electronica Sinica*, vol. 48, no. 4, pp. 734–742, 2020.

[16] Z. Huang, Y. Li, Z. Chen, and L. Liu, "Threshold determination method of Duffing chaotic system based on multi-scale entropy," *Acta Physica Sinica*, vol. 69, no. 16, 2020.

[17] Wang Shi-Yuan, Shi Chun-Fen, Qian Guo-Bing, and Wang Wan-Li, "Prediction of chaotic time series based on the fractional-order maximum correntropy criterion algorithm," *Acta Physica Sinica*, vol. 67, no. 1, p. 018401, 2018.

[18] C. Li, *Prediction and Application of Chaotic Time Series Based on Autoregressive Model*, Chongqing University of Technology, Chongqing, China, 2015.

[19] L. Su, H. Sun, and C. Li, "LL-P-KF hybrid algorithm for detecting and recovering sinusoidal signal in strong chaotic noise," *Acta Electronica Sinica*, vol. 45, no. 4, pp. 844–854, 2017.

[20] L. Su, H. Sun, J. Wang, and L. Yang, "Detection and estimation of weak pulse signal in chaotic background noise," *Acta Physica Sinica*, vol. 66, no. 9, 2017.

[21] L. Su, L. Deng, W. Zhu, and S. Zhao, "Statistical detection of weak pulse signal under chaotic noise based on Elman neural network," *Wireless Communications and Mobile Computing*, vol. 2020, Article ID 9653586, 12 pages, 2020.

[22] M. Sepasi and F. Sassani, "On-line fault diagnosis of hydraulic systems using unscented Kalman filter," *International Journal of Control, Automation and Systems*, vol. 8, no. 1, pp. 149–156, 2010.

[23] H. A. Talebi, K. Khorasani, and S. Tafazoli, "A recurrent neural-network-based sensor and actuator fault detection and isolation for nonlinear systems with application to the Satellite's attitude control subsystem," *IEEE Transactions on Neural Networks*, vol. 20, no. 1, pp. 45–60, 2009.

[24] W. Chine, A. Mellit, V. Lughi, A. Malek, G. Sulligoi, and A. Massi Pavan, "A novel fault diagnosis technique for photovoltaic systems based on artificial neural networks," *Renewable Energy*, vol. 90, pp. 501–512, 2016.

[25] G. Psuj, "Multi-sensor data integration using deep learning for characterization of defects in steel elements," *Sensors*, vol. 18, no. 2, p. 292, 2018.

[26] C. Li, H. Dong, J. Li, and F. Wang, "Distributed Kalman filtering for sensor network with balanced topology," *Systems & Control Letters*, vol. 131, 2019.

[27] X. He, *Research on dietributed decision fusion algorithm under imperfect channels*M.S. Thesis, University of Electronic Science and Technology of China, Szechwan, China.

[28] Iickno Song and S. A. Kassam, "Locally optimum detection of signals in a generalized observation model: the known signal case," *IEEE Transactions on Information Theory*, vol. 36, no. 3, pp. 502–515, 1990.

[29] Iickho Song and S. A. Kassam, "Locally optimum detection of signals in a generalized observation model: the random signal case," *IEEE Transactions on Information Theory*, vol. 36, no. 3, pp. 516–530, 1990.

[30] D. Ciuonzo and P. Salvo Rossi, "Distributed detection of a non-cooperative target via generalized locally-optimum approaches," *Information Fusion*, vol. 30, pp. 261–274, 2017.

[31] D. Ciuonzo and P. S. Rossi, "Quantizer design for generalized locally optimum detectors in wireless sensor networks," *IEEE Wireless Communications Letters*, vol. 7, no. 2, pp. 162–165, 2018.

[32] P. K. Varshney, *Distributed Detection and Data Fusion*, Springer, New York, 1997.

[33] Y. Liu, C. Cheng, and Z. Cui, "Study on optimization of LSFR algorithm in multi-sensor distributed detection," *Transducer and Microsystem Technologies*, vol. 36, no. 3, pp. 21–24, 2017.

[34] D. Li, S. Kar, F. E. Alsaadi, and etc, "Distributed Bayesian quickest change detection in sensor networks via two-layer large deviation analysis," in *2016 54th Annual Allerton Conference on Communication, Control, and Computing (Allerton)*, pp. 1274–1281, Monticello, IL, USA, 2016.

[35] X. Cheng, D. Ciuonzo, and P. S. Rossi, "Multibit decentralized detection through fusing smart and dumb sensors based on Rao test," *IEEE Transactions on Aerospace and Electronic Systems*, vol. 56, no. 2, pp. 1391–1405, 2020.

[36] D. Ciuonzo, S. H. Javadi, A. Mohammadi, and P. S. Rossi, "Bandwidth-constrained decentralized detection of an unknown vector signal via multisensor fusion," *IEEE Transactions on Signal and Information Processing over Networks*, vol. 6, pp. 744–758, 2020.

[37] Z. Yu, "Multi-sensor fusion algorithm based on high-order spherical-radial criterion," *Journal of Detection Control*, vol. 40, no. 5, pp. 26–30, 2018.

[38] H. Zayyani, F. Haddadi, and M. Korki, "Double detector for sparse signal detection from one-bit compressed sensing measurements," *IEEE Signal Processing Letters*, vol. 23, no. 11, pp. 1637–1641, 2016.

[39] X. Wang, G. Li, and P. K. Varshney, "Detection of sparse signals in sensor networks via locally most powerful tests," *IEEE Signal Processing Letters*, vol. 25, no. 9, pp. 1418–1422, 2018.

[40] X. Wang, G. Li, and P. K. Varshney, "Distributed detection of weak signals from one-bit measurements under observation model uncertainties," *IEEE Signal Processing Letters*, vol. 26, no. 3, pp. 415–419, 2019.

[41] L. Su, M. Li, S. Zhao, and T. Xie, "Distributed sensor local linear fusion detection of weak pulse signal in chaotic background," *Journal of Sensors*, vol. 2021, Article ID 6661142, 11 pages, 2021.

[42] F. Takens, "Detecting strange attractors in turbulence," in *Lecture Notes in Mathematics*, Springer, 1981.

[43] J. Lin, Y. Wang, Z. Huang, and Z. Shen, "Speech signals chaos phase space reconstruction time delay multiple-autocorrelation," *Journal of Signal Processing*, vol. 3, pp. 220–225, 1999.

[44] L. Cao, "Practical method for determining the minimum embedding dimension of a scalar time series," *Physica D: Nonlinear Phenomena*, vol. 110, no. 1-2, pp. 43–50, 1997.